 FDMP, vol.14, no.3, pp.155-175, 2018

Numerical Investigation of Combined Surface Radiation and Free Convection in a Square Enclosure with an Inside Finned Heater

Hamici Nadjib[1], Sahi Adel[1, *], Sadaoui Djamel[1] and Djerrada Abderrahmane[1]

Abstract: The study goes further to investigate a two-dimensional numerical model coupling free convection and surface radiation in an air-filled cavity containing a heated thin finned plate. The square enclosure is subjected to isothermal and insulated boundary conditions while the heating element location is varied from the horizontal position (*HPFU*, *HPFD*) to the vertical position (*VPFL*). The dimensionless governing equations under Boussinesq approximations are coupled with a radiative model through the boundaries conditions and solved by the Finite Volume Method. The effects of the pertinent parameters, namely, Rayleigh number ($10^3 \leq Ra \leq 10^6$), fin length ($0.125 \leq L_a \leq 0.875$), fin position ($0.25 \leq H_a \leq 0.75$) and wall emissivity ($0 \leq \varepsilon \leq 1$) are investigated for a constant plate length (A=0.5). Results discussed in terms of streamlines, isotherms, convective and radiative Nusselt numbers highlighted the condition of the heat transfer improvement within the cavity which show an optimal thermal performance for a *VPFL* case (H_a=0.75 and L_a=0.875). Correlations are also developed for convective and Nusselt numbers for H_a=0.25 and L_a=0.5 with a maximum deviation less than 4%.

Keywords: Free convection, surface radiation, square enclosure, thin plate, fin.

Nomenclature

A_i, H_a, L_a	Aspect ratio
h	Length of plate, (m)
H (l_a)	Height of the enclosure (fin), (m)
Cp	Specific heat at constant pressure, (J/kg K)
F	Shape factor
g	Gravitational acceleration, (m/s^2)
J	Dimensionless Radiosity
k	Thermal conductivity, (W/m K)
Nu	Average Nusselt number
N_r	Dimensionless net radiation number, $N_r = \sigma T_H^4 \big/ (k\Delta T / H)$

[1] Laboratoire de Mécanique, Matériaux et Energétique (L2ME), Faculté de Technologie, Université A. Mira de Bejaia, 06000, Bejaia, Algérie.

[*] Corresponding Author: Sahi Adel. Email: sahi.adel@hotmail.fr.

P	Dimensionless pressure $P = pL^2/(\rho\nu^2)$
Pr	Prandtl number, $\Pr = \nu/\alpha$
Q_r	Dimensionless radiative flux density, $Q_r = q_r/(\sigma T_H^4)$
Ra	Rayleigh number, $Ra = g\beta(T_H - T_C)H^3/(\nu\alpha)$
T	Temperature, (K)
V_i	Dimensionless velocity components, $V_i = v_i H/\nu$
X_i	Dimensionless Cartesian coordinates, $X_i = x_i/H$

Greek symbols

P	Density (kg/m^3)
α	Thermal diffusivity (m^2/s)
β	Thermal expansion coefficient (1/K)
μ	Dynamic viscosity (kg/s m)
ν	Kinematic viscosity (m^2/s)
σ	Stefan-Bolzmann constant, W/m^{2}K^4
ε	Emissivity
θ, Θ	Dimensionless temperatures, $\theta = (T - T_C)/(T_H - T_C)$ and $\Theta = T/T_H$
β	thermal expansion coefficient, K^{-1}
ϕ	solid volume fraction
Θ	dimensionless temperature
μ	dynamic viscosity, (kg/ m.s)
δ_{i2}	Delta Kronecker

Subscripts

H, C	Hot, cold
1,2	vertical, horizontal
o	Bottom and top
conv, rad	convection, radiation

1 Introduction

Natural convection heat transfer inside different shaped enclosures has received considerable attention during the last three decades owing to its importance in many practical applications. Some examples may be found in solar collectors, cooling of radioactive waste containers, building heating and ventilation, fire prevention, heat exchangers and electronic cooling devices. The convective motion driven by buoyancy forces has attracted many researchers' interests. A literature survey shows that buoyancy driven phenomena inside different shaped enclosures with various wall boundary conditions have been extensively considered in many research engineering studies; references [Adnani, Meziani, Ourrad et al. (2017); Chen and Cheng (2012); De Vahl Davis (1983); Hamdi, Meziani and Sadaoui (2017); Mobedi (2008); Osario, Avila and Cervantes (2004); Ridouane and Campo (2006)] will give some ideas about fluid flow and thermal characteristics inside cavities with different boundary conditions. All the aforementioned works showed that the heat transfer is limited by the enclosure area and the inclination has an importance on its performance.

The addition of a fin or array of fins to the enclosure surfaces is a suitable technique to improve the overall heat transfer rate between the heat dissipating surfaces and the heat absorbing surfaces. Thorough literature survey revealed that comparatively little work has been reported on natural convection in enclosure with fins attached to its walls [Bilgen (2005); Ghalambaz, Jamesahar, Ismael et al. (2017); Oztop and Bilgen (2006); Paroncini and Corvaro (2009); Tasnim and Collins (2004); Varol, Oztop and Yilmaz (2007)]. These investigations are recently motivated by the advance in the electronics technology, nuclear reactors and the need for reliable and efficient cooling techniques. The results illustrated that the presence of internal fins themselves contributes to the total heat transfer and their presence greatly alter the flow patterns and the fluid temperature adjacent to the enclosure surfaces. Heat transfer rate due to the presence of a fin or array of fins depends greatly on location, material and shape of the fin.

Buoyancy driven flow and heat transfer between body and its surrounding medium has been extensively studied and are greatly influenced by the shape of their cross-section. Many investigations have dealt with the presence of a heating element with various thermal conditions on natural convection within a square enclosure with either a horizontally or vertically imposed temperature difference or heat flux. Available studies deal with natural convective flow and heat transfer around a cylinder inside an enclosure [Xu, Sun, Yu et al. (2009); Yu, Fan, Hua et al. (2010)]. Also, the natural convection heat transfer in the annulus between two concentric or eccentric cylinders, have received considerable attention from researchers in many diverse fields of applications [Larson (1993), Roychowdhury, Das and Sundararajan. (2002)]. The thermal interaction between a cylindrical source and a rectangular enclosure was investigated by Cesini et al. [Cesini, Paroncini, Cortella et al. (1999); Kim, Lee, Ha et al. (2008); Hussain and Hussein (2010)]. The effect of a centered conducting body on natural convection in a square enclosure was investigated by Sun et al. [Sun, Chénier, Lauriat et al. (2011); Muna, Doo, Ha et al. (2016); Sivaraj and Sheremet (2017); Kalidasan and Rajesh Kanna (2017)]. In the light of the above literature, it is pointed out that the detection of the transition threshold from steady-state to time-dependent regimes not only is of basic scientific interest, but also has practical significance. The character of the flow regime, in turn, is expected to affect heat transfer, even if the extent of such an influence remains unpredictable for the time being.

Oztop [Oztop (2004)] studied numerically the effect of the position and the aspect ratio of a thin heated plate on free convection in a cavity to find that Nusselt number increases with Rayleigh and concluded that the enhancement is more pronounced for vertical plate. On the other hand, dealing with laminar free convection in a differentially heated, partitioned, square cavity filled with a heat-generating fluid, Famouri et al. [Famouri and Hooman (2008)] concluded that while fluid friction term has nearly no contribution to entropy production, the heat transfer irreversibility increases monotonically with the Nusselt number and the dimensionless temperature difference. A similar configuration was also considered by Tasnim et al. [Tasnim and Collins (2005)], however, in this study, the shaped plate is adiabatic and arced. The effects of Rayleigh numbers, arc lengths, and shape parameters on heat transfer were discussed. It was concluded that flow and thermal fields are modified by the blockage effect of the baffle. The degree of flow modification due to blockage is enhanced by increasing the shape parameter of the baffle. Altac et al. [Altac and Kurtul (2007)] performed a numerical study of laminar natural convection in tilted rectangular enclosures that contain a vertically hot thin plate. The effect on the flow and heat transfer characteristics of Rayleigh number is investigated parametrically with respect to tilt angle. A useful correlation for practical problems was derived for the averaged Nusselt numbers as a function of Rayleigh and other non-dimensional geometrical parameters.

Saravanana et al. [Saravanana, Abdul Hakeem, Kandaswamy et al. (2008)] made a numerical investigation for two different boundary conditions, isothermal boundary condition and isoflux boundary condition. They found that the resulting convection pattern was stronger for the isothermal boundary condition. A better overall heat transfer can be achieved by placing one of the plates far away from the center of the cavity for isothermal boundary condition and near the center of the cavity for isoflux boundary condition. Recently, Sadaoui et al. [Sadaoui, Sahi, Hamici et al. (2015)] have contributed to the understanding of the flow behavior, through numerical study of the effect of the finned plate on the heat transfer and fluid flow in a square enclosure with isothermal boundary.

The preceding literature review shows that available studies are generally limited to free convection without surface radiation, although this always exists for air-filled enclosures, which can interact strongly with the convection. However, it should further be stated that conjugate thermal radiation with convection in cavities filled with transparent or semitransparent fluid has received considerable attention over the past few decades in view of the numerous potential applications such as thermal insulations, combustion, electronic cooling systems, industrial furnaces, nuclear reactor safety and solar collectors. Reviews on this subject can be found in the publications of Kuznestov et al. [Kuznestov and Sheremet (2009); Nouanegue, Muftoglu and Bilgen (2009); Mondal and Li (2010); Vivek, Sharma and Balaji (2012); Saravanan and Sivaraj (2013, 2015); Li, Bousetta, Chénier et al. (2013); Sahi, Sadaoui, Meziani et al. (2014); Miroshnichenko, Sheremet and Mohamad (2016); Singh and Singh (2016); Sadaoui, Sahi, Djerrada et al. (2016)]. They namely revealed that the surface radiation alters markedly the basic flow pattern in enclosures and thermal performances are affected by the partition configuration. It also found that natural convection heat transfer when coupled with radiation had a greater contribution compared to systems with forced convection. From the revised literature, it can be seen that thermal radiation coupled with natural convection is not as rich as without surface radiation. More, the fluid flow and heat transfer phenomena in the surrounding of a heating element within a square cavity need a more comprehension.

This investigation is dictated by the need to understand the heat transfer mechanisms during cooling of electronic components and printed circuit boards (PCBs) mounted in sealed cabinets whose generated heat must be continuously eliminated in order to maintain their efficiency. However, the resulting heat transfer may be affected by thermal radiation, which is highly dependent on surface properties such as special coatings and surface morphologies of the components and enclosure. Having this in mind, special attention will be paid to the effects of Ra number, surface emissivity, plate orientation, fin length and position on the flow field and heat transfer characteristics in the enclosure.

2 Problem formulation and numerical method

The computational domain is shown in (Fig. 1). The physical model of 2D square cavity filled with a transparent fluid consists of two insulated horizontal walls and two cold vertical walls (T_C) with a hot horizontal finned plate (Fig. 1a) or a hot vertical finned plate T_H (Fig. 1b). All surfaces are assumed gray, diffuse and opaque with an emissivity (ε). In these figures, H shows the height of the enclosure while h and l_a are the width of the thin plate and the fin, respectively. h_1 indicates the distance between the plate and the top wall (Case a), (vertical left wall: Case b), h_2 is the distance from the center of the thin plate to the vertical left wall (Case a) (or top wall: Case b) and h_a is the distance between the fin and the left wall (or top wall: Case b). For simplicity these parameters are defined in terms of aspect ratios such as: $A=h/H$; $A_1=h_1/H$; $A_2=h_2/H$; $H_a=h_a/H$; $L_a= l_a/h$. Throughout the study, the plate length is unchanged such that A=0.5.

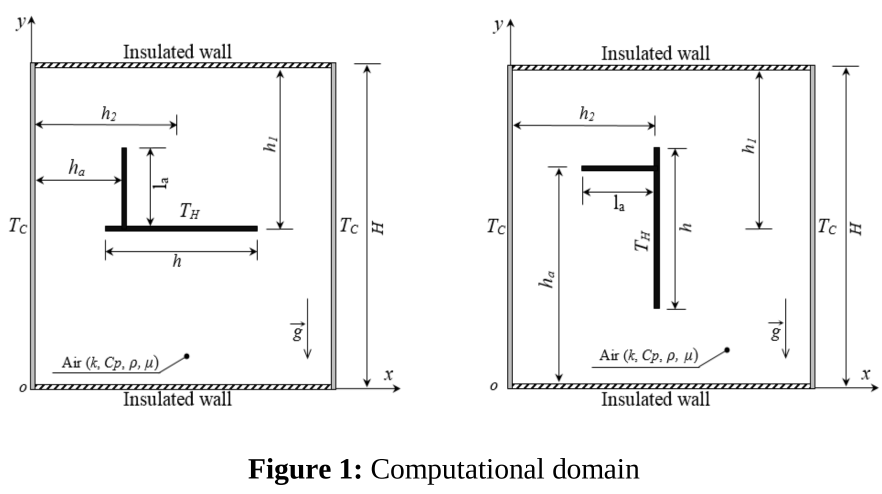

Figure 1: Computational domain

The numerical model for heat transfer and fluid flow in the enclosure was developed under some assumptions as steady, laminar and incompressible Newtonian fluid. Viscous dissipation and compressibility effects are neglected. Also, the fluid properties are assumed constant except the density in the buoyancy terms of the momentum equations, which can be approximated by the Boussinesq approach. The mathematical formulation governing the two-dimensional fluid flow and heat transfer can be written in dimensionless form as:

$$\frac{\partial V_i}{\partial X_i} = 0 \tag{1}$$

$$V_j \frac{\partial V_i}{\partial X_j} = -\frac{\partial P_i}{\partial X_i} + \left(\frac{\partial^2 V_i}{\partial X_j \partial X_j} \right) + \frac{Ra}{\Pr} \theta \delta_{i2} \tag{2}$$

$$V_j \frac{\partial \theta}{\partial X_j} = \frac{1}{\Pr} \left(\frac{\partial^2 \theta}{\partial X_j \partial X_j} \right) \tag{3}$$

Where *Ra* and *Pr* are respectively the Rayleigh and Prandtl number defined by: $Ra = g\beta(T_H - T_C)H^3/(\nu\alpha)$ and $\Pr = \nu/\alpha$. *Ra* gives a measure of the relative importance of buoyancy to viscous and Pr represents the ratio of viscous to thermal diffusivities. In the above equations, *P*, θ are the dimensionless pressure and temperature while X_i and V_i are the dimensionless Cartesians coordinates and corresponding velocity components respectively.

Assuming the non-slip flow, the relevant dimensionless boundary conditions can be written as follows:

$$V_i = 0 \text{ and } \theta = 1 \text{ and } \varepsilon_H = \varepsilon \text{ (inner finned plate)} \tag{4}$$

$$V_i = 0 \text{ and } \theta = 0 \text{ and } \varepsilon_C = \varepsilon \text{ (enclosure vertical walls)} \tag{5}$$

$$V_i = 0 \text{ and } \partial\theta/\partial Y + N_r Q_r = 0 \text{ and } \varepsilon_o = \varepsilon \text{ (horizontal walls)} \tag{6}$$

3 Radiation description

The radiation heat transfer is computed using the radiosity formulation. All the enclosure walls are assumed to be gray, diffuse and opaque with different emissivities. The cavity is filled with a radiatively non-participating fluid (air, Pr=0.71) so only solid surfaces contribute to the radiation exchange. Thus, the radiative heat transfer is made only through the thermal boundary conditions.

The dimensionless radiosity equation for the i^{th} surface of the enclosure (*J*) is defined as:

$$J_i = \varepsilon_i \Theta_i^4 + (1 - \varepsilon_i) \sum_{j=1}^{N} (J_j F_{ij}) \tag{7}$$

So the dimensionless net radiative heat flux ($Q_{r,i}$) along the i^{th} discrete surface is determined by:

$$Q_{r,i} = J_i - \sum_{j=1}^{N}(J_j F_{ij}) \quad \text{i=1,....,N} \tag{8}$$

Where (N) is the number of total radiative surfaces along the boundaries of the enclosures, ε_i the emissivity of the i^{th} surface while the shape factor F_{ij} from the i^{th} element to the j^{th} element of the enclosure are determined using Hottel's crossed string method Hottel and Saroffim (1967).

To determine heat transfer characteristics at the enclosure walls, contributions of both convection and radiation should be taken into account. The mean Nusselt number, which is of a greater interest in engineering applications, is used to evaluate the rate heat transfer on enclosure surfaces. Thus, the global average Nusselt number along the cold wall is defined as the sum of convective and radiative Nusselt-numbers.

$$Nu = Nu_{conv} + Nu_{rad} = -\int_0^1 \frac{\partial \theta}{\partial X} dY + \int_0^1 N_r Q_r dY \tag{9}$$

4 Numerical procedure

The equations of continuity, momentum and energy balance Eqs. (1-3) with the specified boundary conditions (Eqs. (4-6)), are solved numerically by the finite volume method under uniform grid system in x and y directions (Fig. 2). The solver specified uses a pressure correction based on iterative SIMPLER algorithm. The advective terms are discretized using a QUICK scheme whereas a second-order central difference scheme is applied for the diffusion terms (for more details, see Patankar [Patankar (1980)]. To check the convergence of the sequential iterative solution, the normalized residual is calculated for the mass, momentum and energy equations; respectively the convergence is obtained when the residuals become smaller than 10^{-7}.

4.1 Grid independency and validation

To ensure a grid independency a grid testing is performed using various grid combinations (41×41 to 201×201) for the case of natural convection in a cavity with a finned plate as mentioned in Fig. 2 (L_a=0.5 ; H_a=0.5 and A_1=A_2=0.5).

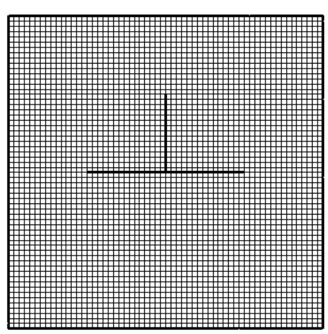

Figure 2: Detail of the computational grid

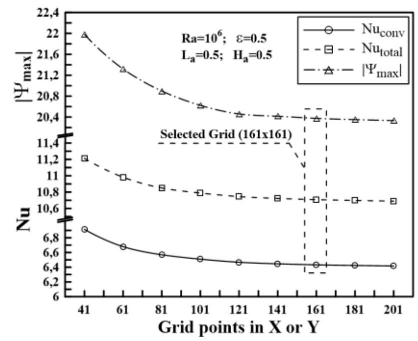

Figure 3: Grid independency (Ra=10^6, L_a=0.5, H_a =0.5 and ε=0.5)

Table 1: Comparison between current work and Saravanan et al. [Saravanan and Sivaraj (2013)]

Ra	ε		Horizontal plate (HP)			Vertical plate (VP)		
			Nu_{conv}	Nu_{rad}	Nu_{total}	Nu_{conv}	Nu_{rad}	Nu_{total}
10^6	0	Saravanan and Sivaraj (2013)	5.2804	0	5.2804	7.6062	0	7.6062
		Current work	5.1718 (2.057%)	0	5.1718 (2.057%)	7.5316 (0.981%)	0	7.5316 (0.981%)
	0.5	Saravanan and Sivaraj (2013)	5.5537	3.3155	8.8696	7.1637	4.1842	11.3479
		Current work	5.4925 (1.102%)	3.2900 (0.769%)	8.7825 (0.982%)	7.0678 (1.339%)	4.1851 (0.022%)	11.2529 (0.837%)
	1	Saravanan and Sivaraj (2013)	5.8533	6.9885	12.8418	6.6731	10.1914	16.8645
		Current work	5.8090 (0.757%)	6.9195 (0.987%)	12.7285 (0.882%)	6.5756 (1.461%)	10.1633 (0.276%)	16.7389 (0.745%)
10^5	0	Saravanan and Sivaraj (2013)]	3.3339	0	3.3339	4.2789	0	4.2789
		Current work	3.2440 (2.697%)	0	3.2440 (2.697%)	4.1848 (2.199%)	0	4.1848 (2.199%)
	1	Saravanan and Sivaraj (2013)	3.4533	3.2436	6.7000	3.8688	4.6860	8.5548
		Current work	3.3798 (2.128%)	3.1711 (2.235%)	6.5508 (2.227%)	3.7763 (2.391%)	4.6544 (0.674%)	8.4307 (1.451%)
10^7	0	Saravanan and Sivaraj (2013)	8.7997	0	8.7997	13.8560	0	13.8560
		Current work	8.7341 (0.745%)	0	8.7326 (0.763%)	13.7333 (0.886%)	0	13.7333 (0.886%)
	1	Saravanan and Sivaraj (2013)	9.9721	15.1241	25.0963	11.9337	21.9862	33.9199
		Current work	10.0845 (1.127%)	14.9586 (1.094%)	25.0431 (0.212%)	11.6641 (2.259%)	21.9185 (0.308%)	33.5826 (0.994%)

Note. The values in ( ) are the absolute difference in %.

For each mesh, maximum stream function (Ψ_{max}) and mean Nusselt number (Nu) for Ra=10^6; ε_H=ε_C=ε_o=ε=0.5 are estimated and presented in Fig. 3. Throughout this investigation, Ψ_{max} and Nu remain almost the same for grids finer than 141×141 and heavily depends on the grid size for less finer grids. Hence, considering both the accuracy and the computational costs, most computations reported in the current work were performed with a multiple grid system of 161×161 leading a maximum deviation less than 3%.

Extensive validations of the developed code for combined convection and surface radiation in a square cavity with a heated plate inside as considered by Saravanan et al. [Saravanan and Sivaraj (2013)]. The simulations have been performed in terms of convective, radiation and total Nusselt number. As listed in Tab. 1, the comparisons are in good agreements (maximum deviation of 2.5%) providing sufficient confidence in present computations.

5 Results and discussion

Such as this investigation is dictated by the need to understand the heat transfer mechanisms during conjugate natural convection and surface radiation in a square cavity with a finned plate, several scenarios were explored. Results to be reported in the following sections are obtained for a Rayleigh number ranging between 10^3 to 10^6 and different aspect ratio (A=0.5; A_1=A_2=0.5, L_a=0.25 to 0.75 and H_a=0.25 to 0.75) while the Prandtl number is kept constant Pr=0.71. All surfaces were considered with the same emissivity varying from ε=0 (no radiative heat exchange) and ε=1 (perfect absorption and emission black surface).

5.1 Temperature and fluid patterns

Buoyancy driven flow and temperature fields inside the enclosure are given by means of streamlines and isotherms. The circulation force of the flow within the cavity takes place by virtue of thermal buoyancy which is represented by the Rayleigh number *Ra*. Fig. 4 illustrates the effect of *Ra* on the flow pattern and temperature distribution in the enclosure for horizontal and vertical plate (*HPFU*, *HPFD* and *VPFL*), respectively. All other parameters (L_a, ε and H_a) were kept constant. As seen, due to linearly heated in the core region and gets blocked at the top adiabatic wall, then flows down along the cooled walls showing two major cells with clockwise and anti-clockwise rotations. Increasing temperature gradient (Ra=10^6) generates faster recirculation rolls: *HPFU* (Ra=10^3, Ψ_{max}=0.1760-Ra=10^6, Ψ_{max}=21.1771). In horizontal configurations (*HPFU* and *HPFD*) it can be seen clearly that each primary cell consists of two co-rotating secondary cells at the top and bottom corners of the enclosure. Moreover, for H_a=0.5 the symmetric boundary conditions produce a symmetric behaviour (streamlines and isotherms) with respect to the vertical axis.

Isothermal lines extending between the cold surfaces are normal to the insulated walls in accordance with the literature without surface radiation. For relatively low Grash of numbers (Ra>10^4), the isotherms plots are smooth curves indicating that the conduction mechanism is dominant. The distributions of isotherms are almost invariant.

However, the increase in the Rayleigh number ($Ra \geq 10^5$) caused by the increased buoyancy forces alters the flow pattern. The temperature contours are distorted so that isothermal plumes appear in the top region. It is clearly observed that the buoyancy strength induces the increasing vortices for $10^4 < Ra \leq 10^6$, this is owing to the dominating influence of the convective current in the cavity. Thus, increasing (Ra) promotes the convection heat transfer mechanism against conduction.

The streamlines and isotherms structures change with the variation of the fin length and position. Indeed the effects of both dimensionless shape parameters (L_a) and (H_a) on the flow pattern and temperature distribution are illustrated in Fig. 5. As noted above, the flow consists of two large cells extending along the cold walls.

In the horizontal case and H_a=0.5, the flow patterns consist of two similar and symmetric counter-rotating cells close to each of the cold walls with respect to the vertical axis of the cavity. As fin height increases (L_a=0.25; 0.5 and 0.75) the intensity of the natural convection increases in *HPFD* case (L_a=0.25: Ψ_{max}=23.2886; L_a=0.75: Ψ_{max}=19.8357) and decreases in *HPFU* case (L_a=0.25: Ψ_{max}=24.7057; La=0.75: Ψ_{max}=28.9070). Unlike the previous case (H_a=0.5) where streamlines and isotherms are symmetric, when decreasing H_a (H_a=0.25) the left primary cell is squeezed by the core of the right primary cell and moves up (*HPFD*) or down (*HPFU*) as L_a grows ($0.25 \leq L_a \leq 0.75$). In *VPFL*, two dominant buoyancy induced vortices prevail in the enclosure, the right as the left one rotate in the clockwise and in counter-clockwise directions, respectively. Increasing Ha (displacement of the fin upwards leads to slow down the fluid flow so its strength decreases (L_a=0.25: Ψ_{max}=26.149; 24.4586; 20.9398; L_a=0.75: Ψ_{max}=30.75725; 27.4119; 17.6125). The opposite phenomenon is observed when increasing the fin length (H_a=0.25: Ψ_{max}=26.1490; 27.074; 30.7572). This generates a multi-cell structure, by splitting the left main cell under the fin displacement.

The isotherms are affected by the presence of the fin so that isothermal plumes appear in the upper part of the cavity highlighting a strong heat transfer in this region. Thermal plumes are located in the middle of the plate (*HPFD*), above it (*VPFL*) or follow the position of the fin (*HPFU*). Moreover, the temperature contours are denser and compressed toward isothermal fined plate and along a large part of the cold walls.

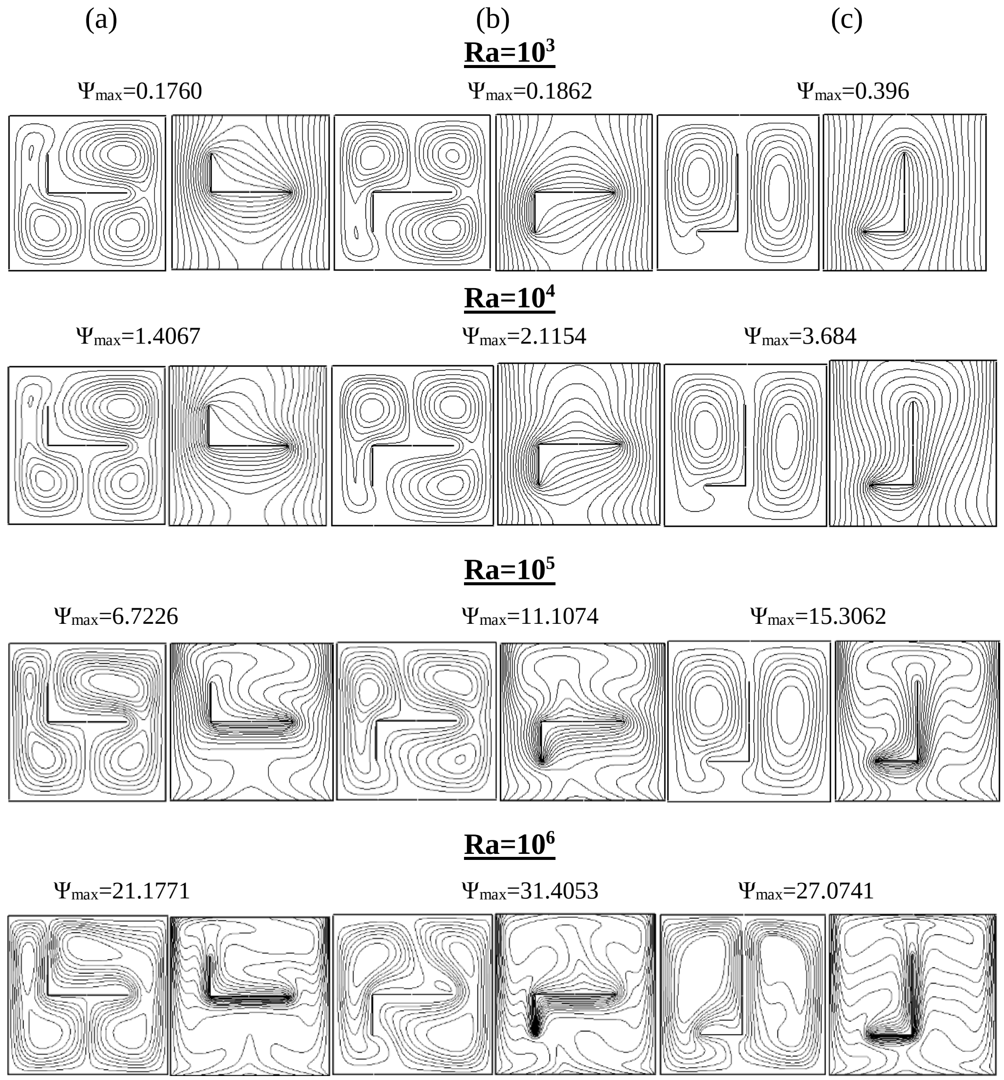

Figure 4: Streamlines (left) and Isotherms (right) and for L_a=0.5, ε=1, H_a=0.25 and different *Ra*. (a) Horizontal finned plate facing up (*HPFU*) (b) Horizontal finned plate facing down (*HPFD*) (c) Vertical finned plate facing left (*VPFL*)

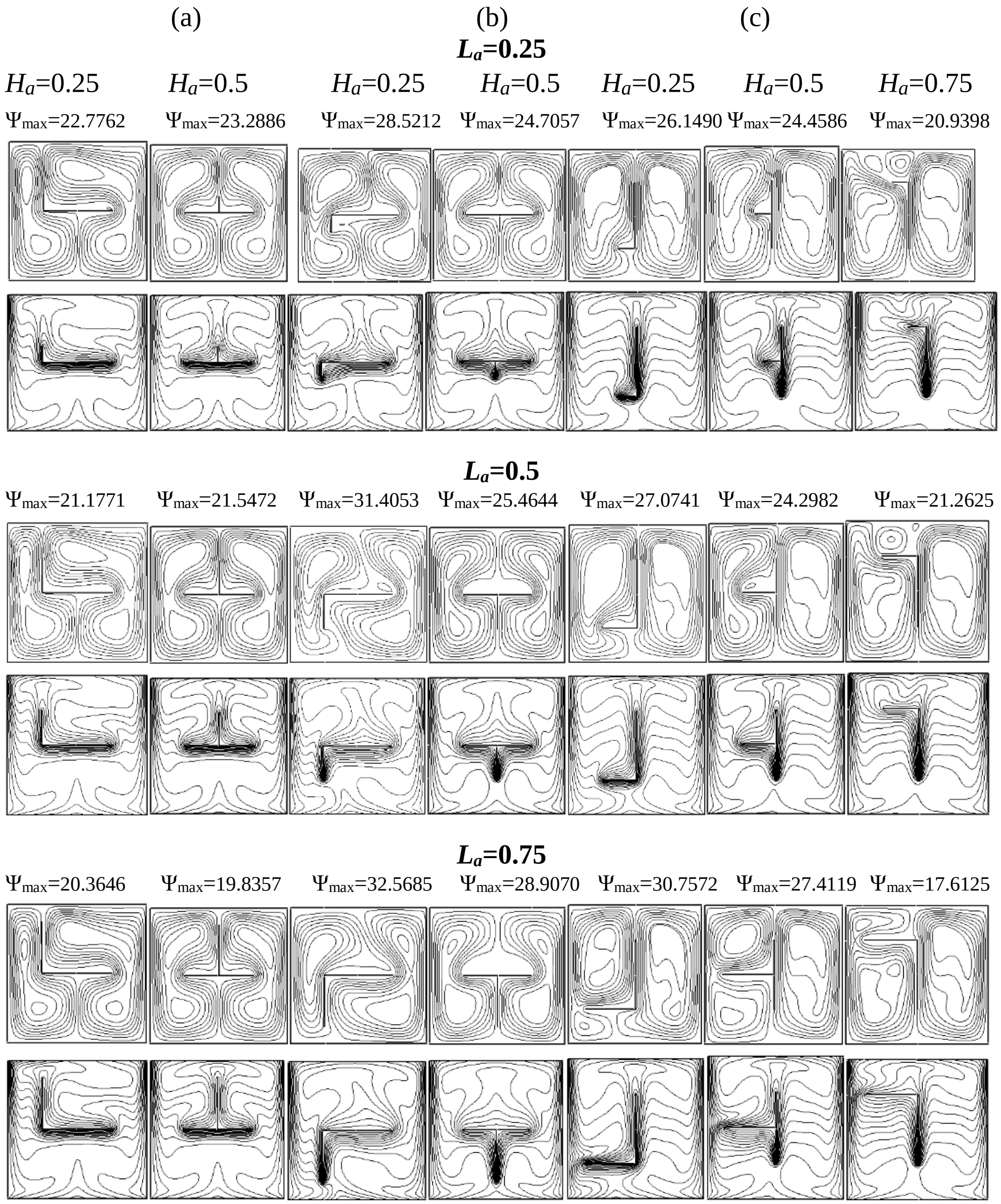

Figure 5: Streamlines and isotherms for $Ra=10^6$, $\varepsilon=1$: L_a= 0.25-0.75 and H_a=0.25-0.75. (a) Horizontal finned plate facing up (*HPFU*) (b) Horizontal finned plate facing down (*HPFD*) (c) Vertical finned plate facing left (*VPFL*)

The Fig. 6 also allows us to analyze the surface radiation effect on the isotherms and the streamlines shape inside the enclosure when $Ra=10^6$, $L_a=0.5$ and $H_a=0.25$. It is clear that the surface radiation for the emissivity has minimal effect on the streamlines except a slight acceleration of the fluid in *HPFD* case.

However, it has a significant effect on the isotherms. As expected, a slight variation in emissivity affects the temperature plots near the insulated walls. Indeed, without surface radiation (ε=0), the isothermal lines are vertical to the insulated walls, while for (ε≠0) isotherms appear more inclined in accordance with the boundary conditions model.

Note that the additional radiative heat exchange introduced by the thermal boundary conditions promotes the development of thermal plumes and thus the global heat exchange.

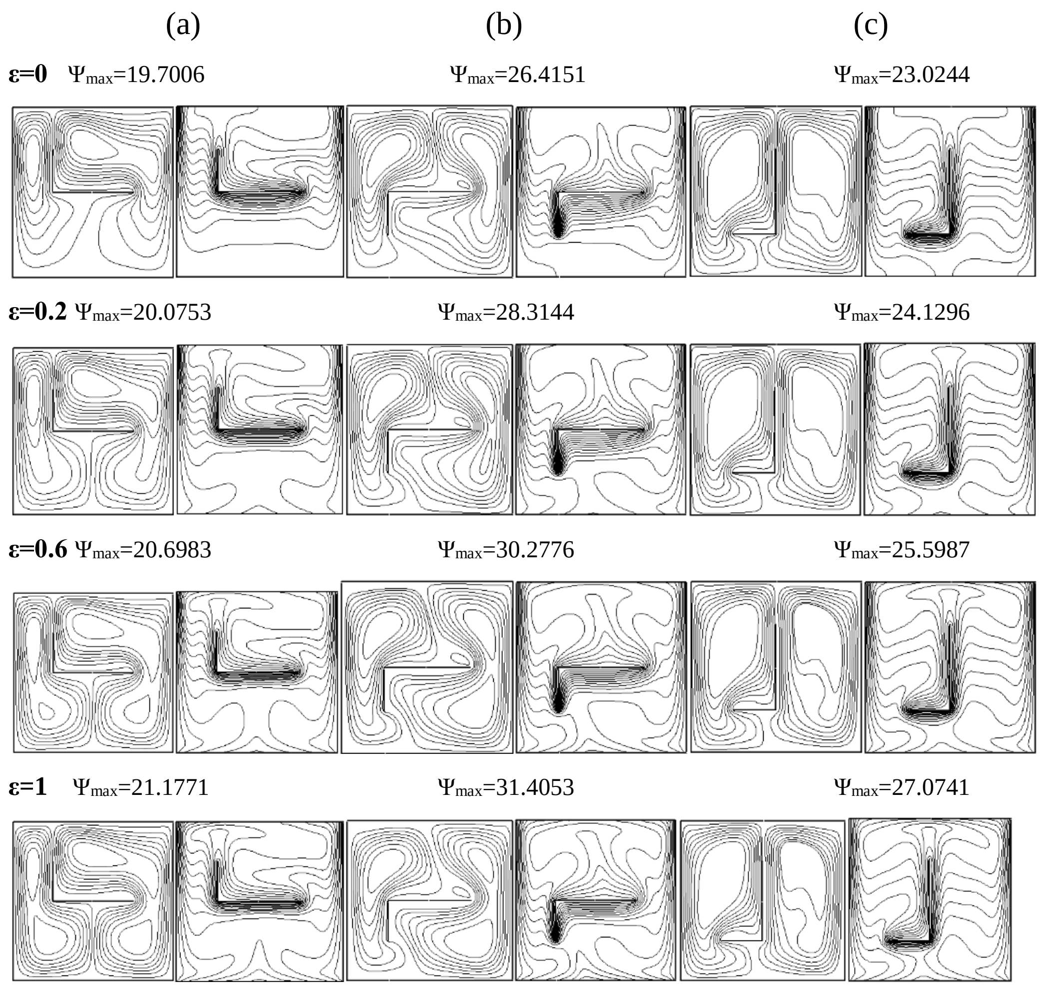

Figure 6: Streamlines (left) and Isotherms (right): Ra=10^6, L_a=0.5, H_a=0.25 and ε=0 to 1. (a) Horizontal finned plate facing up (*HPFU*) (b) Horizontal finned plate facing down (*HPFD*) (c) Vertical finned plate facing left (*VPFL*)

5.2 Heat transfer analysis

The rate of heat transfer is presented in terms of mean Nusselt number calculated by integrating the local Nusselt distribution along the left cold wall as illustrated in Figs. 7 and 8 and Tab. 2.

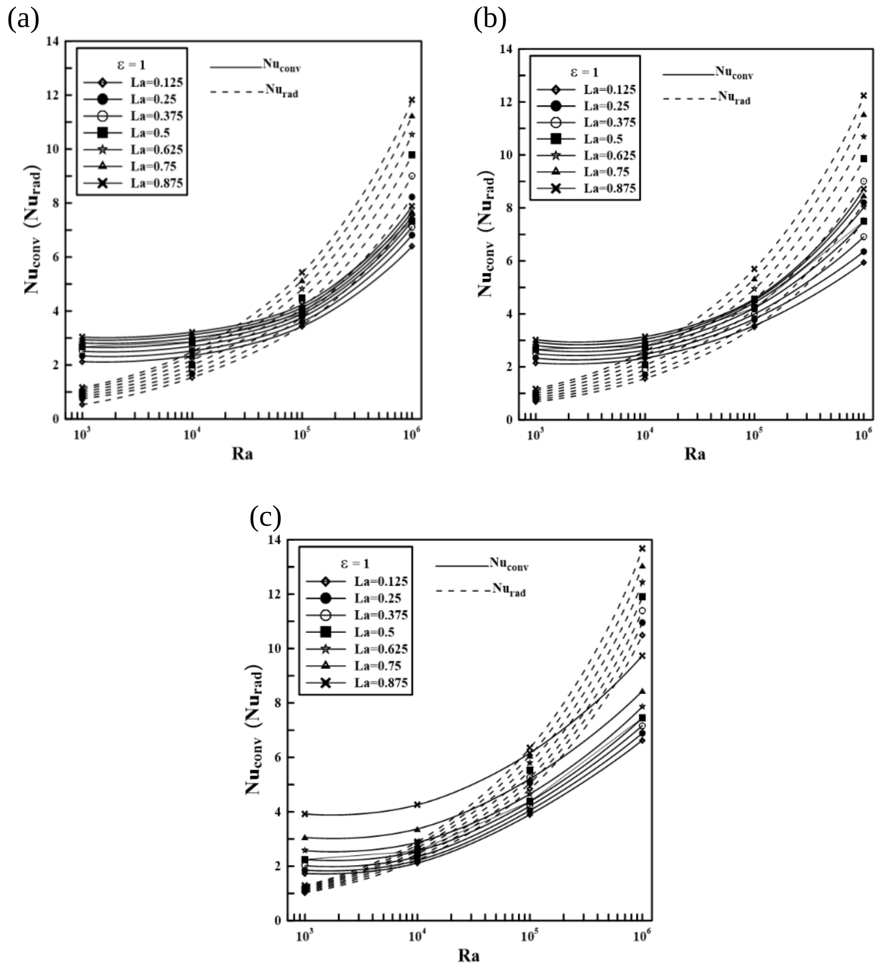

Figure 7: Effects of *Ra* and L_a on Nu_{conv} and Nu_{rad} (H_a=0.25 and ε=1). (a) Horizontal finned plate facing up (*HPFU*) (b) Horizontal finned plate facing down (*HPFD*) (c) Vertical finned plate facing left (*VPFL*)

To highlight the effects produced by changing the fin heights (L_a) on the heat transfer Figs. 7a-7c depict the mean convective (Nu_{conv}) and radiative (Nu_{rad}) Nusselt numbers for different Rayleigh numbers (*Ra*). This allows us to see that the heat transfer (Nu_{conv}) remains substantially unchanged for low Rayleigh values (i.e. when the conduction regime dominates $Ra \leq 10^4$) regardless the considered configuration (*HP* or *VP*). Also, when the heat transfer is mainly due to convection ($Ra > 10^4$), increasing Rayleigh number produces the higher buoyancy-induced flow within the enclosure, consequently the higher convective Nusselt number. Furthermore, it is noted that (Nu_{conv}) depends closely on the length of the fin, so for a fixed *Ra* the convective Nusselt number increases with the increase of L_a.

However, in diffusion regime and for $L_a \leq 0.625$ *HPFU* and *HPFD* cases produce the same effect on the heat transfer rate while in *VPFL*, Nu_{conv} values are less important. This trend is reversed for largest L_a (L_a=0.75 and 0.875). When convection prevails in the cavity ($Ra>10^4$), *VPFL* case shows better results than the *HPFD* followed by the *HPFU* case, respectively (i.e.: L_a=0.875: Nu_{conv}=10.75 (*VPFL*); 8.75 (*HPFD*); 7.85 (*HPFU*).

The contribution of the heat exchange by radiation (Nu_{rad}) in the overall heat transfer is very important as indicated in the same Figs. (7a-7c). Examination of these figures indicates that the increase in the flow regime (*Ra*) causes a significant contribution of radiative exchanges, as well as the increase in the length of the fin affects the radiative Nusselt number for all considered cases. In addition, *VPFL* allows better radiative exchanges than *HP* cases, which give substantially the same results. It will also be noted that radiative Nusselt number is greater than the convective Nusselt number for large values of Rayleigh number ($Ra \geq 10^4$: Heat transfer mainly due to convection), the opposite phenomenon is observed for lowest values (conduction dominates). This is particularly verified for largest fin lengths.

Figs. 8a-8c depicts the effect of surface emissivity (cold, hot and insulated walls) on the averaged convective and radiative Nusselt numbers. As shown, walls emissivity has little effects on Nu_{conv} which remains substantially unchanged. Whereas, the radiative Nusselt number is very sensitive to the emissivity, such that the contribution of the radiative exchanges increases with the increase of the emissivity (especially for highest *Ra*). Further, for almost considered *Ra* ($10^3 \leq Ra < 10^6$) Nu_{conv} is greater than Nu_{rad} when considering gray surfaces ($\varepsilon<1$). According to same figure, radiative heat exchanges at the surfaces in *VP* configuration are more significant compared to those of the other cases (*HP*).

Moreover, Nu_{rad} and Nu_{conv} for the three configurations can be correlated pretty well with the Rayleigh number and the emissivity for a maximum deviation less than 1% and 4%, respectively as follows:

$$\mathrm{Nu_{rad}} = \mathrm{C_0} \cdot \varepsilon^{\mathrm{C_1}} \cdot \mathrm{Ra}^{\mathrm{C_2} - \mathrm{C_3} \cdot \mathrm{C_4^{\varepsilon}}} \tag{10}$$

$$\mathrm{Nu_{conv}} = \mathrm{D_0} \cdot e^{\frac{\mathrm{D_1}}{\varepsilon + \mathrm{D_2}}} \left(\mathrm{Ra} - \mathrm{D_3} - \mathrm{D_4} e^{\mathrm{D_5} \cdot \varepsilon}\right)^{\mathrm{D_6} \cdot e^{\frac{\mathrm{D_7}}{\varepsilon + \mathrm{D_8}}}} \tag{11}$$

Where coefficients C_i and D_i are given as follows:

	C_0	C_1	C_2	C_3	C_4
HPFU	0.08581	1.16535	0.34198	0.00863	0.00827
HPFD	0.09132	1.16726	0.33816	0.01509	2.96E-05
VPFL	0.11711	1.21017	0.33402	0.03263	1.46E-08

	D_0	D_1	D_2	D_3	D_4	D_5	D_6	D_7	D_8
HPFU	0.08639	0.0451	0.25525	-54574.7	18387.83	-0.45988	0.32159	-0.01426	0.26093
HPFD	0.16751	0.05805	0.28438	-20394	4203.084	-1.6089	0.27677	-0.02564	0.32826
VPFL	0.2535	-0.02589	0.55661	-11696.2	7020.274	-0.1791	0.24937	-67.419E-5	-0.50648

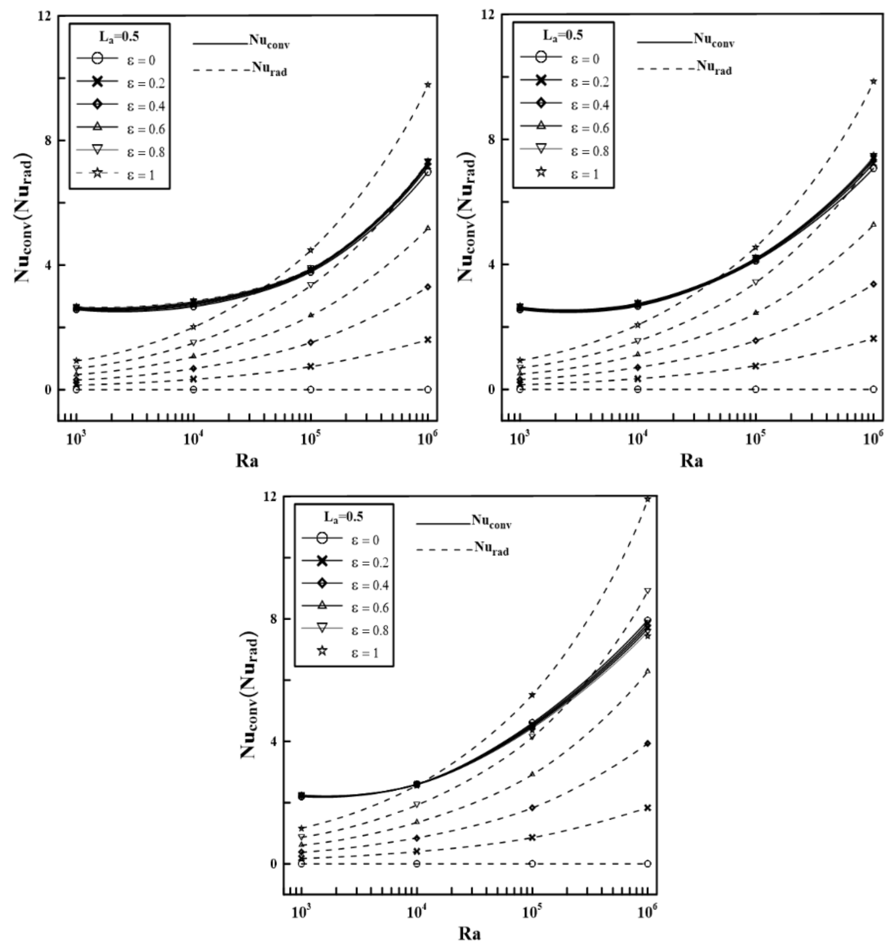

Figure 8: Effects of *Ra* and ε on Nu_{conv} and Nu_{rad} (H_a=0.25; L_a=0.5). (a) Horizontal finned plate facing up (*HPFU*) (b) Horizontal finned plate facing down (*HPFD*) (c) Vertical finned plate facing left (*VPFL*)

As summarized in Tab. 2 an increase of the shape parameters (L_a and ε) improve the convective heat transfer (Nu_{conv}) in *HPFU* case. However, for largest values of L_a (L_a>0.5) no significant effect is noticed on (Nu_{conv}) when increasing (ε). Whereas in (*HPFD*) case and (H_a≥0.5; L_a≥0.5), the convective Nusselt number decreases with the increase of the surface emissivity. Furthermore, in *VP* case (excepted when L_a=0.875) the convective Nusselt number decreases with the increase of (ε).

Finally, still from Tab. 2 in *VP* case, Nu_{rad} for H_a=0.25 is larger followed by H_a=0.75 and H_a=0.5, respectively whereas Nu_{rad} in *HP* case is more important for lowest H_a (H_a=0.25).

Table 2: Effect of (ε), (L_a) and (H_a) on Nu_{conv} and Nu_{rad} for Ra=10^6

			L_a=0.125		L_a=0.375		L_a=0.625		L_a=0.875	
			Nu_{conv}	Nu_{rad}	Nu_{conv}	Nu_{rad}	Nu_{conv}	Nu_{rad}	Nu_{conv}	Nu_{rad}
HPFU	H_a=0.25	ε=0	5,693	0	6,661	0	7,262	0,000	7,581	0
		ε=0.5	6,126	3,507	6,989	3,978	7,490	4,415	7,825	4,750
		ε=1	6,391	7,546	7,115	9,000	7,511	10,536	7,878	11,836
	H_a=0.5	ε=0	5,175	0	5,905	0	6,603	0,000	6,976	0
		ε=0.5	5,506	3,429	6,101	3,974	6,719	4,552	7,128	4,983
		ε=1	5,761	7,066	6,146	8,341	6,678	9,931	7,135	11,193
	H_a=0.75	ε=0	5,189	0	6,005	0	6,659	0	6,995	0
		ε=0.5	5,461	3,521	6,179	4,086	6,820	4,633	7,206	5,100
		ε=1	5,749	7,330	6,317	8,509	6,888	9,797	7,275	10,982
HPFD	H_a=0.25	ε=0	5,426	0	6,508	0	7,653	0	8,612	0
		ε=0.5	5,707	3,521	6,776	4,026	7,930	4,543	8,685	4,985
		ε=1	5,948	7,512	6,912	9,008	8,023	10,696	8,721	12,231
	H_a=0.5	ε=0	5,157	0	6,137	0	7,350	0	8,250	0
		ε=0.5	5,556	3,436	6,455	3,971	7,421	4,539	8,118	5,015
		ε=1	5,823	7,064	6,507	8,303	7,345	9,888	7,995	11,277
	H_a=0.75	ε=0	5,289	0	6,163	0	7,319	0	8,249	0
		ε=0.5	5,633	3,530	6,254	4,040	7,190	4,563	8,054	5,057
		ε=1	5,945	7,379	6,327	8,454	7,137	9,674	7,966	10,904
VPFL	H_a=0.25	ε=0	7,427	0	7,775	0	8,184	0	9,492	0
		ε=0.5	7,035	4,378	7,475	4,838	8,035	5,313	9,649	5,816
		ε=1	6,606	10,499	7,147	11,395	7,823	12,435	9,688	13,689
	H_a=0.5	ε=0	7,083	0	7,186	0	7,561	0	9,187	0
		ε=0.5	6,714	4,301	6,942	4,638	7,484	5,063	9,461	5,501
		ε=1	6,215	10,121	6,527	10,466	7,231	11,379	9,499	12,644
	H_a=0.75	ε=0	7,517	0	7,777	0	7,939	0	9,215	0
		ε=0.5	7,282	4,345	7,522	4,732	7,860	5,148	9,465	5,496
		ε=1	6,906	10,429	7,233	11,217	7,779	12,139	9,551	13,060

6 Conclusion

Coupled free convection and surface radiation in an air-filled cavity containing a heated thin finned plate has been numerically treated. Effect of several parameters such as the length and position of the fin, the orientation of the plate and surface radiation for *Ra* ranging between 10^3 and 10^6 with Pr=0.71 have been examined. The obtained results highlighted the effect of the above-mentioned parameters on flow structure, temperature distribution and heat transfer rate. The contribution of convection to the global heat exchanges rate is proportional to *Ra* number and fin length. Moreover, considering surface radiation does not affect the transition conduction-convection. The radiative heat transfer rate grows with the surface emissivity, especially in vertical plate case and highest *Ra* values. Further, its contribution is less important compared to convection when considering gray surfaces. The convective heat transfer (Nu_{conv}) remains substantially unchanged for low Rayleigh values (conduction dominating) and grows with the Rayleigh number (convection prevailing). The flow remains steady state until Ra=10^6 beyond instabilities appear. The overall heat transfer rate is improved using longer fin with vertical plate, whereas it is reduced in horizontal case. Thus, the optimal thermal performances were obtained for a fin positioned on the upper end of the vertical plate (H_a=0,75; L_a=0,875).

References

Adnani, M.; Meziani, B.; Ourrad, O.; Zitoune, M. (2017): Natural convection in a square cavity: Numerical study for different values of prandtl number. *Fluid Dynamics & Materials Processing*, vol. 12, no. 1, pp. 1-14.

Altac, Z.; Kurtul, O. (2007): Natural convection in tilted rectangular enclosures with a vertically situated hot plate inside. *Applied Thermal Engineering*, vol. 27, no. 11-12, pp. 1932-1840.

Bilgen, E. (2005): Natural convection in cavities with a thin fin on the hot wall. *International Communications in Heat and Mass Transfer*, vol. 48, no. 17, pp. 3493-3505.

Cesini, G.; Paroncini, M.; Cortella, G.; Manzan, M. (1999): Natural convection from a horizontal cylinder in a rectangular cavity. *International Communications in Heat and Mass Transfer*, vol. 42, no. 10, pp. 1801-1811.

Chen, C. L.; Cheng, C. H. (2012): Numerical predictions of natural convection with liquid fluids contained in an inclined arc-shaped enclosure. *International Communications in Heat and Mass Transfer*, vol. 39, no. 2, pp. 209-215.

De Vahl Davis, G. (1983): Natural convection of air in a square cavity: A benchmark numerical solution. *International Journal for Numerical Methods in Fluids*, vol. 3, no. 3, pp. 249-264.

Famouri, M.; Hooman, K. (2008): Entropy generation for natural convection by heated partitions in a cavity. *International Communications in Heat and Mass Transfer*, vol. 35, no. 4, pp. 492-502.

Ghalambaz, M.; Jamesahar, E.; Ismael, M. A.; Chamkha, J. (2017): Fluid-structure interaction study of natural convection heat transfer over a flexible oscillating fin in a square cavity. *International Journal of Thermal Sciences*, vol. 111, pp. 256-273.

Hamdi, M.; Meziani, B.; Sadaoui, D. (2017): Numerical study of mixed convection and flow pattern in various across-shape concave enclosures. *International Journal of Heat and Technology*, vol. 35, no. 33, pp. 567-575.

Hottel, H.; Saroffim, A. F. (1967): *Radiative Heat Transfer*. Mc Graw Hill, USA.

Hussain, S. H.; Hussein, A. K. (2010): Numerical investigation of natural convection phenomena in a uniformly 2 heated circular cylinder immersed in square enclosure filled with air at different vertical locations. *International Communications in Heat and Mass Transfer*, vol. 37, no. 8, pp. 1115-1126.

Kalidasan, K.; Rajesh Kanna, P. (2017): Natural convection on an open square cavity containing diagonally placed heaters and adiabatic square block and filled with hybrid nanofluid of nanodiamond-cobalt oxide/water. *International Communications in Heat and Mass Transfer*, vol. 81, pp. 64-71.

Kim, B. S.; Lee, D. S.; Ha, M. Y.; Yoon, H. S. (2008): A numerical study of natural convection in a square enclosure with a circular cylinder at different vertical locations. *International Communications in Heat and Mass Transfer*, vol. 51, no. 7-8, pp. 1888-1906.

Kuznestov, G. V.; Sheremet, M. A. (2009): Conjugate natural convection with radiation in an enclosure. *International Journal of Heat and Mass Transfer*, vol. 52, no. 9-10, pp. 2215-2223.

Larson, D. W.; Gartling, D. K.; Schimmel, W. P. (1993): Natural convection studies in nuclear spent-fuel shipping casks: Computation and experiment. *Journal of Energy*, vol. 2, no. 3, pp. 147-154.

Li, R.; Bousetta, M.; Chénier, E.; Lauriat, G. (2013): Effect of surface radiation on natural convective flows and onset of flow reversal in asymmetrically heated vertical channels. *International Journal of Thermal Sciences*, vol. 65, pp. 9-27.

Miroshnichenko, I. V.; Sheremet, M. A.; Mohamad, A. A. (2016): Numerical simulation of a conjugate turbulent natural convection combined with surface thermal radiation in an enclosure with a heat source. *International Journal of Thermal Sciences*, vol. 109, pp. 172-181.

Mobedi, M. (2008): Conjugate natural convection in a square cavity with finite thickness horizontal walls. *International Communications in Heat and Mass Transfer*, vol. 35, no. 4, pp. 503-513.

Mondal, B.; Li, X. (2010): Effect of volumetric radiation on natural convection in a square cavity using lattice boltzmann method with non-uniform lattices. *International Journal of Heat and Mass Transfer*, vol. 53, no. 21-22, pp. 4935-4948.

Muna, G. S.; Doo, J. H.; Ha, M. Y. (2016): Thermo-dynamic irreversibility induced by natural convection in square enclosure with inner cylinder. Part-i: Effect of tilted angle of enclosure. *International Communications in Heat and Mass Transfer*, vol. 97, pp. 1102-1119.

Nouanegue, H. F.; Muftoglu, A.; Bilgen, E. (2009): Heat transfer by natural convection, conduction and radiation in an inclined square enclosure bounded with a solid wall. *International Journal of Thermal Sciences*, vol. 48, no. 5, pp. 871-880.

Osario, A.; Avila, R.; Cervantes, J. (2004): On the natural convection of water near its density inversion in an inclined square cavity. *International Communications in Heat and Mass Transfer*, vol. 47, no. 19-20, pp. 4491-4495.

Oztop, H.; Bilgen, E. (2006): Natural convection in differentially heated and partially divided square cavities with internal heat generation. *International Journal of Heat and Fluid Flow*, vol. 27, no. 3, pp. 466-475.

Oztop, H. F.; Dagtekin, I.; Bahloul, A. (2004): Comparison of position of a heated thin plate located in a cavity for natural convection. *International Communications in Heat and Mass Transfer*, vol. 31, no. 1, pp. 121-132.

Paroncini, M.; Corvaro, F. (2009): Natural convection in a square enclosure with a hot source. *International Journal of Thermal Sciences*, vol. 48, no. 9, pp. 1683-1695.

Patankar, S. V. (1980): *Numerical Heat Transfer and Fluid Flow*. Hemisphere Publishing Corporation, USA.

Ridouane, E. H.; Campo, A. (2006): Free convection performance of circular cavities having two active curved vertical sides and two inactive curved horizontal sides. *Applied Thermal Engineering*, vol. 26, no. 17-18, pp. 2409-2416.

Roychowdhury, D. G.; Das, S. K.; Sundararajan, T. S. (2002): Numerical simulation of natural convective heat transfer and fluid flow around a heated cylinder inside an enclosure. *Heat Mass Transfer*, vol. 38, no. 7-8, pp. 565-576.

Sadaoui, D.; Sahi, A.; Djerrada, A.; Mansouri, K. (2016): Coupled radiation and natural convection within an inclined sinusoidal solar collector heated from below. *Mechanics & Industry*, vol. 17, no. 3, pp. 302-311.

Sadaoui, D.; Sahi, A.; Hamici, N.; Meziani, B.; Amoura, T. (2015): Free convection in a square enclosure with a finned plate. *Mechanics & Industry*, vol. 16, no. 13, pp. 310-317.

Sahi, A.; Sadaoui, D.; Meziani, B.; Mansouri, K. (2014): Effects of thermal boundary conditions, surface radiation and aspect ratio on thermal performance in "T" shallow cavity. *Mechanics & Industry*, vol. 15, no. 6, pp. 557-568.

Saravanan, S.; Sivaraj, C. (2013): Combined natural convection and thermal radiation in a square cavity with a nonuniformly heated plate. *International Journal of Heat and Fluid Flow*, vol. 40, pp. 54-64.

Saravanan, S.; Sivaraj, C. (2015): Combined natural convection and thermal radiation in a square cavity with a nonuniformly heated plate. *Computers & Fluids*, vol. 117, pp. 125-138.

Saravanana, S.; Abdul Hakeem, A. K.; Kandaswamy, P.; Leeb, J. (2008): Buoyancy convection in a cavity with mutually orthogonal heated plates. *Computers and Mathematics with Applications*, vol. 55, no. 12, pp. 2903-2912.

Singh, D. K.; Singh, S. N. (2016): Combined free convection and surface radiation in tilted open cavity. *International Journal of Thermal Sciences*, vol. 107, pp. 111-120.

Sivaraj, C.; Sheremet, M. A. (2017): Mhd natural convection in an inclined square porous cavity with a heat conducting solid block. *Journal of Magnetism and Magnetic Materials*, vol. 426, pp. 351-360.

Sun, H.; Chénier, E.; Lauriat, G. (2011): Effect of surface radiation on the breakdown of steady natural convection flows in a square, air-filled cavity containing a centred inner body. *Applied Thermal Engineering*, vol. 31, no. 6-7, pp. 1252-1262.

Tasnim, S. H.; Collins, M. R. (2004): Numerical analysis of heat transfer in a square cavity with a baffle on the hot wall. *International Communications in Heat and Mass Transfer*, vol. 35, no. 5, pp. 639-650.

Tasnim, S. H.; Collins, M. R. (2005): Suppressing natural convection in a differentially heated square cavity with an arc shaped baffle. *International Communications in Heat and Mass Transfer*, vol. 31, no. 1-2, pp. 94-106.

Varol, Y.; Oztop, H. F.; Yilmaz, T. (2007): Natural convection in triangular enclosures with protruding isothermal heater. *International Journal of Heat and Mass Transfer*, vol. 50, no. 13-14, pp. 2451-5462.

Vivek, K.; Sharma, A. M.; Balaji, C. (2012): Interaction effects between laminar natural convection and surface radiation in tilted square and shallow enclosures. *International Journal of Thermal Sciences*, vol. 60, pp. 70-84.

Xu, X.; Sun, G.; Yu, X.; Hub, Y.; Fa, L. et al. (2009): Numerical investigation of laminar natural convective heat transfer from a horizontal triangular cylinder to its concentric cylindrical enclosure. *International Journal of Heat and Mass Transfer*, vol. 52, no. 13-14, pp. 3176-3186.

Yu, Z. T.; Fan, L. W.; Hua, Y. C.; Cen, K. F. (2010): Prandtl number dependence of laminar natural convection heat transfer in a horizontal cylindrical enclosure with an inner coaxial triangular cylinder. *International Journal of Heat and Mass Transfer*, vol. 53, no. 7-8, pp. 1333-1340.